JOURNAL OF MATERIALS SCIENCE 32 (1997) 4679–4686

As*K*-edge EXAFS study of the ternary system Sb_2S_3–As_2S_3–Tl_2S

J.-M. DURAND*, J. OLIVIER-FOURCADE, J.-C. JUMAS
Laboratoire de Physicochimie des Matériaux Solides (URA 407 CNRS), Université Montpellier II – Sciences et Techniques du Languedoc, Place Eugène Bataillon, 34095 Montpellier Cedex 5, France

M. WOMES
Laboratoire de Spectroscopie Atomique et Ionique (URA 775 CNRS), Université de Paris Sud, Bât 350, 91405 Orsay Cedex, France

P. PARENT
L.U.R.E., Université Paris Sud, Bât. 309 D, 91405 Orsay Cedex, France

The local environment of arsenic atoms in vitreous samples of the system Sb_2S_3–As_2S_3–Tl_2S has been studied by EXAFS at the As*K*-edge. The crystalline compound $Tl_{5.6}As_{15}S_{25.3}$ situated within the zone of glass formation of the Sb_2S_3–As_2S_3–Tl_2S phase diagram was used as reference compound in order to derive appropriate phase and amplitude functions. The structure parameters determined were the number of first neighbours N_{As-S}, the arsenic-sulphur distance, R_{As-S}, and the Debye-Waller factor, σ_{As-S}. The influence of the glass-forming antimony sulphide Sb_2S_3 and the glass-modifying thallium sulphide Tl_2S on the As_2S_3 host matrix has been shown.

1. Introduction

There is currently increasing interest in chalcogenide glasses owing to their optical properties (transparency in the infrared, optical fibres) and their applications in informatics (electronic switches, optical memories) [1–8]. Besides the optical properties determining their technical applications, the mechanical and thermal properties of these glasses are of equally high importance, because they determine the possibilities to handle and machine these materials.

However, optical and mechanical properties are not always coupled to the same structural parameter. Some properties, like electronic conductivity or infrared transparency, are influenced by short-range order, whilst others like hardness, thermal stability or elasticity, are rather determined by long-range order.

Although chalcogenide glasses nowadays belong to the most currently studied materials with regard to possible applications in the domain of optics, there is still little known about the relationship between composition or structure, on the one side, and their properties, on the other. Several models have been developed, the bases of which vary from disordered lattices to molecular clusters, in order to describe the relationship structure–properties [9–13]. Which of these models gives the best results depends on the type of glass considered. In the case of the binary system Sb_2S_3–As_2S_3, especially, two different hypotheses are discussed controversially: (i) a complete phase separation with pure Sb_2S_3 and As_2S_3 phases, and (ii) a single-phased disordered lattice where arsenic is randomly substituted by antimony.

Kawamoto and Tsuchibashi [14] pointed out that infrared and X-ray scattering spectra of glasses of the system Sb_2S_3–As_2S_3 were a simple superposition of the spectra of the pure Sb_2S_3 and As_2S_3 phases. However, in order to explain the results of experiments where glasses were dissolved in concentrated hydrochloric acid, they suggest the presence of As–S–Sb bridges connecting the two phases. They propose a glass morphology with a continuous As_2S_3 lattice containing isolated domains of the Sb_2S_3 phase. A similar model has been established by White *et al.* [15] who explain the fact that molten arsenic-rich phases cannot be recrystallized, by the low diffusion rate of antimony in the As_2S_3 phase. The antimony atoms remain thus isolated and prevent the formation of the As_2S_3 lattice. Tichy *et al.* [16] found a linear relation between the optical gap and the concentration of As_2S_3 in the glass. They proposed considering compounds of the Sb_2S_3–As_2S_3 system as an ideal solid solution of microstructural unities of As_2S_3 and Sb_2S_3.

Bychkov and Wortmann [17] studied the system Sb_2S_3–As_2S_3 by ^{121}Sb Mössbauer spectroscopy. They found a linear decrease of the isomer shift with decreasing concentration of Sb_2S_3, which was

*Author to whom all correspondence should be addressed.

interpreted as an increase of the Sb–S bond lengths with decreasing antimony concentration. From their results, they suggested the formation of a disordered, glass-like network where arsenic is randomly substituted by antimony.

In this paper, we report the results of a study of the Sb_2S_3–As_2S_3–Tl_2S system by extended X-ray absorption fine structure (EXAFS) spectroscopy at the arsenic *K*-edge. As the number of intense synchrotron radiation sources dedicated to X-ray absorption experiments has increased during recent years, EXAFS has become a powerful tool in the fields of crystallography and material science. It allows determination of the number of neighbours of the absorbing atom, the bond lengths between absorber and neighbours, and it gives information on the distribution of the bond lengths due to structural or thermally induced disorder.

In contrast to As_2S_3 and Sb_2S_3, which are both glass-forming compounds, Tl_2S is a glass-modifying compound. EXAFS allows it to be decided whether the As_2S_3 and Sb_2S_3 phases are completely separated or whether arsenic is randomly substituted by antimony. In the first case, EXAFS at the As*K*-edge would show a rather composition-independent distribution of As–S distances, mainly caused by thermally induced vibrations, while in the second case the presence of As–S–As, as well as As–S–Sb bridges, should modify the distance distribution, depending on the antimony concentration.

2. Experimental procedure

The amorphous samples were synthesized in two steps. First the binary sulphides Sb_2S_3, As_2S_3 and Tl_2S were prepared by direct reaction from stoichiometric mixtures of the elements in evacuated tubes ($p = 10^{-3}$ Pa). Then, mixtures of these binary sulphides were heated in evacuated tubes up to about 1173 K for 1 h under permanent shaking, and then quenched in a mixture of water, ice, and salt. Finally, the glasses were kept for 2 d at a temperature 50 K below that of their respective glass transition temperature, in order to stabilize the glasses. This procedure minimizes mechanical strain caused by quenching.

X-ray diffraction with CuK_α radiation revealed that all samples were amorphous. The diffraction patterns showed no sharp and intense Bragg reflection, but several scattering fringes. Additionally, the thermal properties of the samples, like the glass transition temperature, T_g, the crystallization temperature, T_c, and the melting temperature, T_m, were measured by differential thermal analysis, which also proved that the synthesis led to amorphous compounds (Table I).

EXAFS data at the arsenic *K*-edge were recorded using the synchrotron radiation of DCI storage ring in Orsay. The beam line was equipped with a Si (3 1 1) double monochromator. The second monochromator crystal was slightly mistuned in order to suppress harmonics. The samples were finely ground, sieved to 5 μm and then homogeneously dusted on to Kapton adhesive tape.

TABLE I Thermal properties of the vitreous compounds of the ternary system Sb_2S_3–As_2S_3–Tl_2S. The glass transition temperature, T_g, the crystallization temperature, T_c, and the melting temperature, T_m, were measured. The two last temperatures (T_c and T_m) were not determined for arsenic-rich vitreous compounds. These compounds cannot easily be recrystallized [15]

Samples	Sb_2S_3 (%)	As_2S_3 (%)	Tl_2S (%)	T_g (K)	T_c (K)	T_m (K)
1A	75	25	0	494	549	765
2A	50	50	0	486	614	687
3A	25	75	0	484	–	–
4A	0	100	0	481	–	–
5A	0	90	10	442	–	–
6A	0	80	20	426	–	–
7A	0	72.8	27.2	415	–	–
8A	0	60	40	405	497	549
9A	0	50	50	397	447	576
20A	65	15	20	470	533	670
21A	50	30	20	466	568	627
22A	35	45	20	463	–	–
23A	20	60	20	455	–	–
24A	5	75	20	439	–	–
30A	40	20	40	432	472	658
31A	20	40	40	420	496	574
32A	10	50	40	411	502	536

3. Data analysis

The data were evaluated on a micro-computer using Michalowicz's EXAFS program [18]. The EXAFS signal was extracted from the rough data in the following way: (i) a spline polynome simulating atomic absorption was fitted to the pre-edge part of the spectrum, extrapolated to the whole energy range covered by the spectrum and then subtracted from the rough data, (ii) the EXAFS signal $\chi(E)$ was calculated using the method of Lengeler–Eisenberger [19], (iii) E_0, the ionization threshold energy of the photoelectron, was chosen in the vicinity of the inflection point of the main absorption step (11 864 eV).

Up to this point, the EXAFS signal, χ (Fig. 1), is given as a function of energy, $\chi(E)$. In order to turn to a spectrum being a function of wave vectors k, $\chi(k)$, we may use the relation

$$k = \left[\frac{2\, m_e \pi^2 (E - E_0)}{h^2}\right]^{1/2} \tag{1}$$

with m_e the electron mass, h Planck's constant, E the kinetic energy of the out-going photoelectron, and E_0 the ionization threshold energy.

This leads to a spectrum of the form

$$\chi(k) = \frac{\mu(k) - \mu_1(k)}{\mu_1(k) - \mu_0(k)} \tag{2}$$

with $\mu(k)$ the experimental absorption spectrum, $\mu_0(k)$ the base line, and $\mu_1(k)$ the atomic absorption. The spectrum $\chi(k)$ was cut off smoothly below 25 and above 130 nm^{-1} using a Kaiser window ($\tau = 2.5$) and then weighted by multiplying it with k^3. This new data set allows us to turn from the reciprocal space of wavevectors to real space by means of Fourier transformation, leading to a new spectrum directly scaled in distances (nm) . From this spectrum we may now select a range of interest. In our case we filtered out the

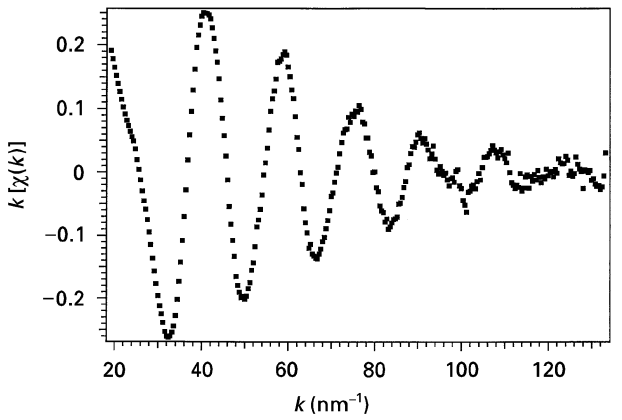

Figure 1 EXAFS signal of the vitreous compound 3A (25% Sb_2S_3–75% As_2S_3).

intense peak present in the spectra of all samples, representing the first coordination sphere of sulphur atoms around the absorbing arsenic atom. With this peak filtered, we have seven independent parameters, N_{ind}, according to Shannon's theorem

$$N_{ind} = \frac{2\,\Delta k\,\Delta R}{\pi} \tag{3}$$

Thus, six parameters may be refined independently from each other. The numerical refinement is based on the general theoretical expression describing the EXAFS signal within the approximations of plane waves and single scattering

$$k\chi(k) = -S_0^2 \sum_i \frac{N_i}{R_i^2}\, e^{-2k^2\sigma_i^2}\, e^{[2R_i/\lambda(k)]} \times f_i(\pi, k)\, \sin[2kR_i + \Phi_i(k)] \tag{4}$$

$$\lambda(k) = \frac{1}{\Gamma}\left[\left(\frac{\eta}{k}\right)^4 + k\right]$$

with i representing the ith sphere of neighbours, N_i the number of neighbours in the ith sphere, R_i the distance between absorber and the ith sphere, σ_i the Debye–Waller factor describing structural disorder (distribution of distances around a mean value, existence of different sites or defects in local stoichiometry) as well as disorder due to thermally excited phonons. Γ is a constant related to the mean free path of the outgoing photoelectron, η is a parameter allowing to adjust the mean free path at k values below 30 nm^{-1} and S_0^2 is a general scale factor. $\Phi_i(k)$ and $f_i(\pi, k)$ are, respectively, phase and amplitude functions of the back-scattered photoelectron and may be taken from tables such as those of Teo and Lee [20] or McKale *et al.* [21] or may be derived experimentally from reference compounds.

The experiments and the analysis of the data were made with great care.

4. Results and discussion

4.1. Choice of the reference compound

One of the most important points of an EXAFS study is the proper choice of the reference compound, in order to determine appropriate phase and amplitude functions $\Phi_i(k)$ and $f_i(\pi, k)$ for the each pair of absorber and neighbour atom to be studied.

In the ternary system Sb_2S_3–As_2S_3–Tl_2S, four crystalline compounds can be found, which may serve as reference compounds: As_2S_3 [22], $Tl_{5.6}As_{15}S_{25.3}$ [23], $TlAsS_2$ [24], and Tl_3AsS_3 [25] (Fig. 2). In all four cases, the crystal structures, atomic positions and bond lengths are well known from X-ray diffraction.

Arsenic is always found in a pyramidal environment AsS_3E consisting of three nearest neighboured sulphur atoms and the lone pair of As $4s^2$ electrons, usually denoted E. In Tl_3AsS_3, arsenic occupies only one crystallographic site with three equal As–S distances of 0.223 nm [25]. In As_2S_3, arsenic is found on two different sites with As–S bond lengths varying from 0.224 to 0.231 nm and a mean $\bar{R}_{As-S}$ of 0.228 nm [22]. There are also two crystallographically different arsenic sites in $TlAsS_2$, with bond lengths varying from 0.208–0.232 nm and $\bar{R}_{As-S} = 0.225$ nm [24]. In $Tl_{5.6}As_{15}S_{25.3}$ we have to deal with five different arsenic sites with As–S distances varying from 0.216–0.252 nm and $\bar{R}_{As-S}$ of 0.229 nm [23].

Envelopes of the EXAFS signal [26] were determined for all compounds. These functions were then compared to the envelopes of the EXAFS signal of several amorphous samples. Best agreement between the envelopes of the EXAFS signal of amorphous and crystalline compounds was found for $Tl_{5.6}As_{15}S_{25.3}$. This result might be surprising, because $Tl_{5.6}As_{15}S_{25.3}$ seems to be less apt as a reference compound due to its rather complicated crystalline structure with five different arsenic sites. $Tl_{5.6}As_{15}S_{25.3}$ is, however, the only crystalline compound, which is well situated within the zone of glass formation and not on its boundaries, like As_2S_3 or $TlAsS_2$ or outside, like Tl_3AsS_3.

$Tl_{5.6}As_{15}S_{25.3}$ was thus chosen as reference compound.

4.2. Crystalline compounds (system As_2S_3–Tl_2S)

Let us first consider the crystalline compounds. Table II gives the results of the refinement of the

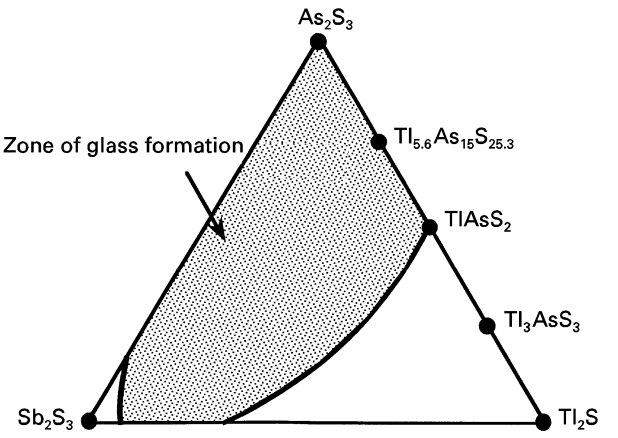

Figure 2 Zone of glass formation in the ternary system Sb_2S_3–As_2S_3–Tl_2S, together with some of the crystalline compounds found within this ternary system.

TABLE II Results of the refinement of the parameters N_{As-S}, R_{As-S}, σ_{As-S}, and E_0 of the crystalline compounds using the phase and amplitude functions of the reference compound. The corresponding values determined by X-ray diffraction are given in parentheses

Crystalline compounds	N_{As-S} ($\pm$ 0.4)	σ_{As-S} ($\pm$ 0.0010 nm)	R_{As-S} ($\pm$ 0.001 nm)	ΔE_0 ($\pm$ 0.9 eV)	Fit ($\times 10^3$)
As_2S_3	3.0	0.0065	0.229 (0.228)	− 2.2	11.7
$TlAsS_2$	3.2	0.0096	0.229 (0.225)	− 0.5	1.7
Tl_3AsS_3	3.3	0.0066	0.226 (0.223)	− 0.4	10.7

EXAFS spectra of the three crystalline compounds As_2S_3, $TlAsS_2$ and Tl_3AsS_3, using the phase and amplitude functions of $Tl_{5.6}As_{15}S_{25.3}$. Good agreement is found for As_2S_3 between the values derived from EXAFS and the results of X-ray diffraction, given in brackets. Stronger deviations between the two data sets are found for $TlAsS_2$ and Tl_3AsS_3. This can be explained by the somewhat shorter As–S distances in these compounds as compared to As_2S_3 and $Tl_{5.6}As_{15}S_{25.3}$, giving bonds of more covalent character. The phase and amplitude functions of the reference compound are thus less apt for these two samples than for As_2S_3, where bond lengths and bond characters are more similar to those of $Tl_{5.6}As_{15}S_{25.3}$.

When the number of nearest neighbours N is fixed at 3, the fit leads to somewhat lower Debye–Waller factors, σ, for $TlAsS_2$ and Tl_3AsS_3, while the distances remain unchanged (Table III). As it is known that arsenic generally obeys the "8-N" rule [27–32], which means that its coordination number is given by the number of electrons needed to fill the valence shell, the parameter N was fixed at 3 for all samples to be discussed in this paper, supposing a pyramidal environment of the AsS_3E type for all compounds.

A further result which can be derived from the study of these few crystalline compounds is the correlation between local disorder and the Debye–Waller factor, σ, which will be helpful for the interpretation of the results obtained for the amorphous samples.

Fig. 3 shows the Fourier transforms of all four crystalline compounds. The first intense peak reflects the first shell of neighbours, while the second less-intense peak at 0.3–0.4 nm is due to the next nearest neighbours. These may be thallium, sulphur or arsenic at very different distances from the absorber atom, so that the evaluation of the Fourier transforms will be restricted to the first peak. As can be seen from Fig. 3, the amplitude of this peak varies considerably from one compound to another. These variations must be due to different Debye–Waller factors, σ, because the number of nearest neighbours has been fixed at 3 for all compounds. The Debye–Waller factor is influenced by bond strengths and atomic mass both numbers determining the phonon spectrum. The bond strength, in turn, is influenced by the bond length. A further important factor is the more or less broad distribution of bond lengths, depending on the number of crystal defaults and on the number of different kinds of nearest and next-nearest neighbours. In particular, this last factor allows the variations of the amplitudes of the Fourier transform in Fig. 3, to be explained. The most intense peak is found for Tl_3AsS_3, where all three sulphur neighbours surrounding the arsenic atom are at the same distance from the absorber and all three are bound to only one arsenic atom giving three non-bridging bonds As–S.

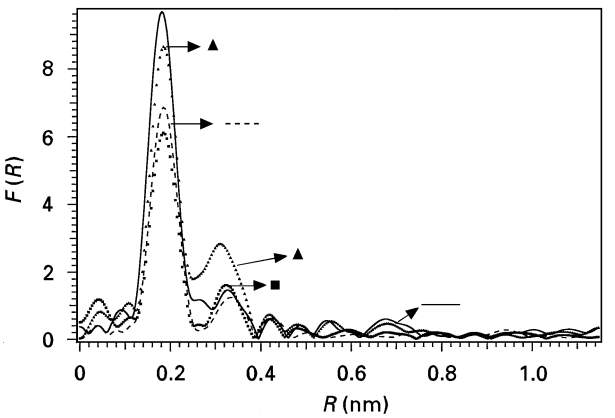

Figure 3 Fourier transforms of the crystalline compounds (▲) As_2S_3, (– – –) $Tl_{5.6}As_{15}S_{25.3}$, (■) $TlAsS_2$, and (——) Tl_3AsS_3.

In As_2S_3, the As–S bonds are homogeneous in so far as all three sulphur neighbours are bound to two arsenic atoms giving three sulphur bridges As–S–As. However, the distribution of As–S distances between 0.224 and 0.231 nm leads to a slightly reduced peak intensity as compared to Tl_3AsS_3. A still lower peak intensity is found for $Tl_{5.6}As_{15}S_{25.3}$ owing to the distribution of the As–S distances on the five different crystallographic arsenic sites, and the lowest intensity of $TlAsS_2$ can be explained by the fact that, besides a distribution of As–S distances, we have to deal with two different kinds of bonds, two sulphur bridges As–S–As and one non-bridging bond As–S per atom. The changes of the Debye–Waller factor can be attributed to variations of distance distribution around a mean value.

The study of these crystalline compounds shows that all crystallographic details are well enough reproduced by EXAFS when the phase and amplitude

TABLE III Results of the refinement of the parameters R_{As-S}, σ_{As-S}, and E_0 of the crystalline compounds with N_{As-S} fixed at 3. The phase and amplitude functions are those of the reference compound

Crystalline compounds	σ_{As-S} ($\pm$ 0.0006 nm)	R_{As-S} ($\pm$ 0.001 nm)	ΔE_0 ($\pm$ 0.9 eV)	Fit ($\times 10^3$)
As_2S_3	0.0066	0.229	− 2.2	11.8
$TlAsS_2$	0.0093	0.229	− 0.5	1.7
Tl_3AsS_3	0.0059	0.226	− 0.4	13.8

functions of $Tl_{5.6}As_{15}S_{25.3}$ are used. This justifies our choice of the reference compound and lets us conclude that the environment of the arsenic atoms will be equally well reproduced for the amorphous samples.

4.3. Amorphous compounds

Let us now turn to the amorphous samples. Fig. 4a shows the positions in the phase diagram of all samples studied in this work. Amorphous samples are denoted by numbers followed by "A", while crystalline samples are given with their chemical formula. The samples are situated in the binary systems As_2S_3–Tl_2S and Sb_2S_3–As_2S_3 as well as in the ternary system Sb_2S_3–As_2S_3–Tl_2S on lines corresponding to constant concentrations of 20 and 40 mol % Tl_2S, as is shown schematically in Fig. 4b.

The results obtained for all amorphous samples with N refined are gathered together in Table IV. The number of first neighbours is equal or close to 3 (3 ± 0.2) for all amorphous compounds, the mean As–S distance varies between 0.228 and 0.230 nm. This shows that even in amorphous compounds, arsenic obeys the "8-N" rule. N may thus be fixed to 3 as for the crystalline samples. This allows to determine Debye–Waller factor σ with higher precision, because σ and N are correlated. The results found for $N = 3$ are given in Table V. The As–S distances remain unchanged with respect to the case where N is refined because these two parameters are uncorrelated. Fig. 5 shows the simulation of the EXAFS oscillations of sample 32A, using the phase and amplitude functions of $Tl_{5.6}As_{15}S_{25.3}$ and fixing N_{As-S} at 3.

All results discussed here refer to the data set with $N = 3$.

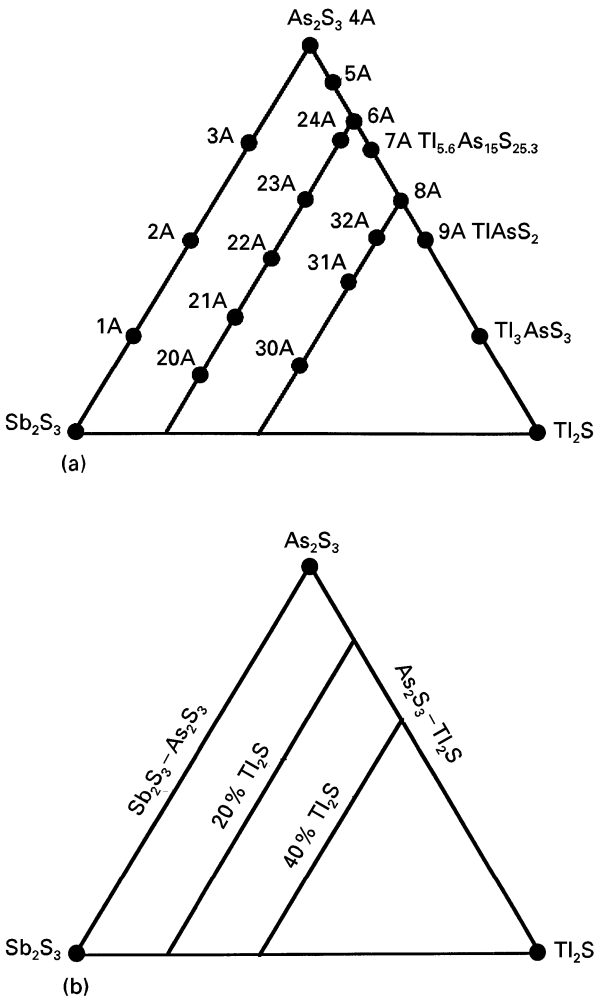

Figure 4 Schematic diagrams of the ternary system Sb_2S_3–As_2S_3–Tl_2S showing the compositions of all amorphous samples studied in this work.

4.3.1. The binary system As_2S_3–Tl_2S

The Fourier transforms of several amorphous samples are shown in Fig. 6. Fig. 7 gives the variation of the Debye–Waller factor with sample composition. The Debye–Waller factor increases with increasing concentration of Tl_2S, leading to more and more reduced intensities of the first Fourier transform peak. The interpretation of this behaviour follows the one given above for the crystalline compounds. The Tl–S bonds are of more ionic character and thus much longer than the As–S bonds. The glass-modifying compound Tl_2S breaks the As–S–As bridges by forming $As\text{–}S^{-\delta}\ldots Tl^{+\delta}$ units, where δ is the partial charge of the ions. The As–S distances in these units are shorter than those in the As–S–As bridges. The number of sulphur bridges As–S–As decreases and the number of non-bridging bonds As–S increases when the thallium concentration is raised. The compound $TlAsS_2$ with two non-bridging bonds per arsenic atom marks the limit of the zone of glass formation. The environment of the arsenic atom thus becomes more and more inhomogeneous when the thallium concentration is raised with longer As–S bonds in the bridges and shorter As–S distances in the non-bridging As–S bonds. This leads to an increase of the Debye–Waller factor and to a decrease of the Fourier transform amplitude. As the number of shorter terminal bonds increases when we reach the limit of the zone of glass formation, we should expect a reduction of the mean As–S bond length when going from vitreous compound As_2S_3 (0.230 nm) to sample 9A (0.228 nm). The results given in Table V show that there is effectively a trend to shorter bonds when the thallium concentration is raised. Our interpretation of the EXAFS spectra is in agreement with the results of Heo *et al.* [33] obtained by XPS and infrared spectroscopy, who also found an increasing number of non-bridging bonds when the thallium concentration is increased.

4.3.2. The binary system Sb_2S_3–As_2S_3

Fig. 8 shows the dependence of the Debye–Waller factor on the Sb_2S_3 concentration. In contrast to the glass-modifying thallium sulphide, the introduction of the glass-forming antimony sulphide into the As_2S_3 host matrix leads to a decreasing σ with increasing concentration of the introduced substituent.

In the preceding section, we attributed the raising Debye–Waller factor to the increasing numbers of broken As–S–As bridges and non-bridging As–S bonds. Here we attribute the effect not to broken As–S–As bridges but rather to a random substitution

TABLE IV Results of the refinement of the parameters N_{As-S}, R_{As-S}, σ_{As-S}, and E_0 of the amorphous compounds using the phase and amplitude functions of the reference compound

Amorphous compounds	N_{As-S} ($\pm$ 0.3)	σ_{As-S} ($\pm$ 0.0008 nm)	R_{As-S} ($\pm$ 0.001 nm)	ΔE_0 ($\pm$ 0.6 eV)	Fit ($\times 10^3$)
1A	2.8	0.0061	0.229	− 0.6	21.6
2A	3.0	0.0068	0.229	− 0.6	7.5
3A	3.2	0.0078	0.229	− 0.4	1.5
4A	3.1	0.0078	0.230	− 0.5	3.0
5A	3.1	0.0082	0.230	− 0.5	1.1
6A	3.1	0.0085	0.229	− 2.0	3.3
7A	3.0	0.0085	0.229	− 1.5	2.6
8A	3.1	0.0090	0.229	− 0.3	1.1
9A	3.0	0.0091	0.228	− 1.9	3.1
20A	3.2	0.0082	0.228	− 1.1	14.2
21A	2.9	0.0070	0.229	− 0.5	6.6
22A	3.0	0.0077	0.229	− 0.5	1.1
23A	3.1	0.0079	0.229	− 0.4	1.7
24A	3.1	0.0086	0.230	− 0.2	0.8
30A	2.8	0.0074	0.228	− 0.3	9.5
31A	2.8	0.0075	0.228	− 0.2	12.5
32A	3.0	0.0085	0.229	− 0.4	0.6

TABLE V Results of the refinement of the parameters R_{As-S}, σ_{As-S}, and E_0 of the amorphous compounds with N_{As-S} fixed at 3. The phase and amplitude functions are those of the reference compound

Amorphous compounds	σ_{As-S} ($\pm$ 0.0005 nm)	R_{As-S} ($\pm$ 0.001 nm)	ΔE_0 ($\pm$ 0.6 eV)	Fit ($\times 10^3$)
1A	0.0066	0.229	− 0.5	23.6
2A	0.0068	0.229	− 0.6	7.5
3A	0.0075	0.229	− 0.5	2.4
4A	0.0077	0.230	− 0.5	3.2
5A	0.0080	0.230	− 0.5	1.4
6A	0.0083	0.229	− 2.0	3.4
7A	0.0085	0.229	− 1.5	2.6
8A	0.0089	0.229	− 0.3	1.3
9A	0.0090	0.228	− 1.9	3.2
20A	0.0069	0.228	0.0	98.7
21A	0.0072	0.229	− 0.5	6.7
22A	0.0076	0.229	− 0.6	1.2
23A	0.0076	0.229	− 0.4	2.3
24A	0.0083	0.230	− 0.3	1.4
30A	0.0078	0.228	− 0.2	10.6
31A	0.0081	0.228	− 0.2	14.8
32A	0.0085	0.229	− 0.5	0.6

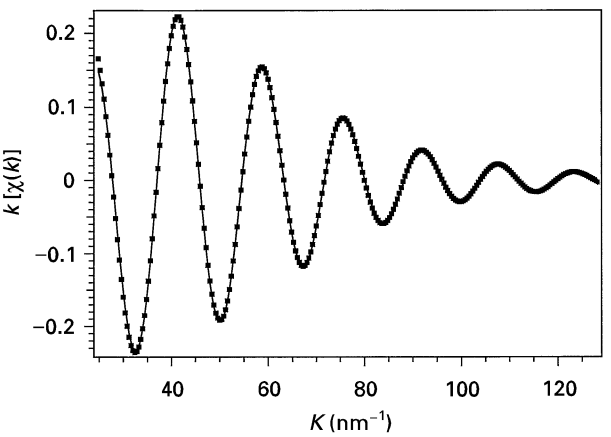

Figure 5 (■) Experimental and (——) calculated EXAFS spectrum of the amorphous compound 32A (10% Sb_2S_3–50% As_2S_3 –40% Tl_2S). The calculation is based on the phase and amplitude function of the reference compound $Tl_{5.6}As_{15}S_{25.3}$.

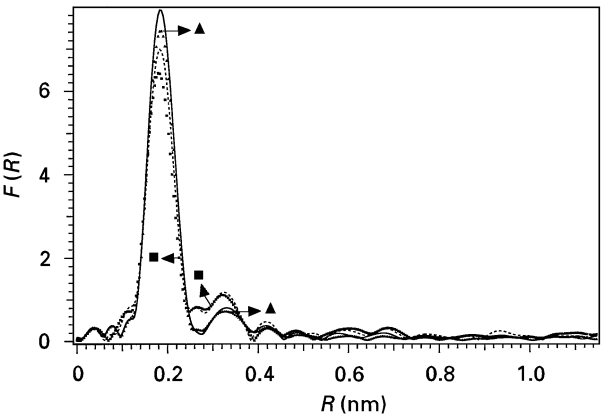

Figure 6 Fourier transforms of several amorphous samples of the As_2S_3–Tl_2S system: (——) 4A, (▲) 5A, (– – –) 6A, (■) 9A.

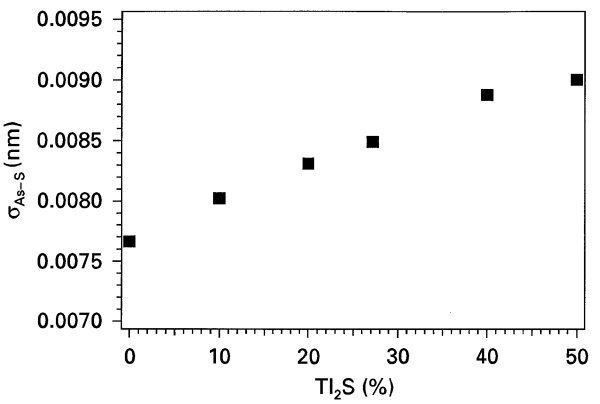

Figure 7 Variation of the Debye–Waller σ_{As-S} factor with composition in the system As_2S_3–Tl_2S.

of arsenic by antimony leading to As–S–Sb bridges. As the Sb–S bonds are more ionic and therefore somewhat longer than the As–S bonds, one may expect, as explained before in the As_2S_3–Tl_2S system, a slight shortening of the As–S bonds involved in these bridges. As can be seen from Table V, there is indeed

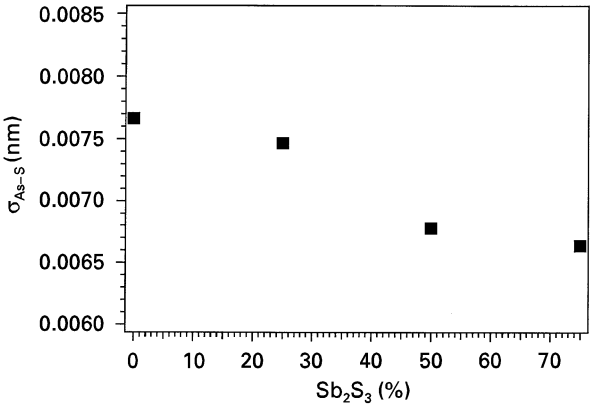

Figure 8 Variation of the Debye–Waller σ_{As-S} factor with composition in the system As_2S_3–Sb_2S_3.

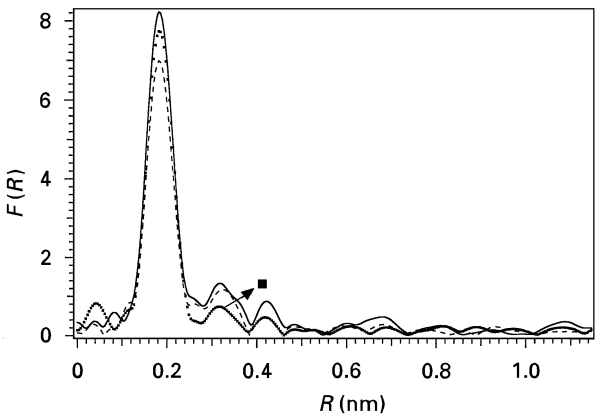

Figure 9 Fourier transforms of several amorphous samples of the Sb_2S_3–As_2S_3–Tl_2S system with a constant Tl_2S concentration of 20 mol %: (——) 21A, (■) 23A, (– – –) 6A.

a tendency to shorter As–S bonds in going from As_2S_3 (0.230 nm) to sample 1A (0.229 nm). These results are in agreement with the ^{121}Sb Mössbauer spectroscopy measurements of Bychkov and Wortmann [17]. They found an increasing Sb–S distance in the Sb_2S_3–As_2S_3 system when the antimony concentration was raised and concluded also a random substitution of arsenic by antimony. From both Bychkov and Wortmann's and our work it may be concluded that As–S–Sb bridges lengthen the Sb–S bonds involved in bridges while they have the inverse effect on As–S bonds. This behaviour is confirmed by other techniques such as XAS at the SbL_{III} and SK-edges [34, 35], and ^{121}Sb Mössbauer, infrared and Raman spectroscopies [36, 37].

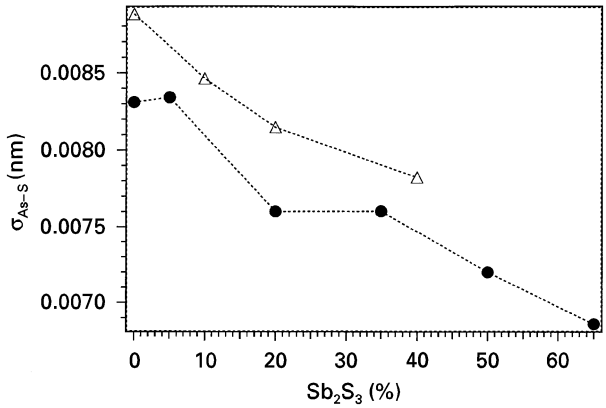

Figure 10 Variation of the Debye–Waller σ_{As-S} factor with composition in the Sb_2S_3–As_2S_3–Tl_2S system with Tl_2S concentrations of (●) 20 and (△) 40 mol %.

4.3.3. The ternary system Sb_2S_3–As_2S_3–Tl_2S

Several samples within the ternary system Sb_2S_3–As_2S_3–Tl_2S with Tl_2S concentrations of 20 and 40 mol % were studied. Fig. 9 shows the Fourier transforms of several samples containing 20 mol % Tl_2S. Fig. 10 shows the dependence of the Debye–Waller factor on the Sb_2S_3 amount contained in the host matrix for both concentrations of thallium sulphide. As already observed in the As_2S_3–Tl_2S, the higher amount of Tl_2S leads to higher Debye–Waller factors due to the increased numbers of broken As–S–As bridges and non-bridging As–S bonds. The Debye–Waller factors decrease in both cases when antimony is introduced. The increasing antimony concentration leads thus to a gradual formation of As–S–Sb bridges and diminishes the number of non-bridging As–S bonds. This should lead to a shortening of the mean As–S distance, as explained in the preceding sections. The results in Table V show that there is effectively a tendency to shorter As–S distances when the antimony concentration is raised. A recent EXAFS study at the SbL_{III}-edge [34] showed, however, that in contrast to the binary system Sb_2S_3–As_2S_3, the antimony coordination number in the ternary system can be higher than 3. The hypothesis of a simple substitution of arsenic by antimony is therefore not valid in the case of the ternary system.

5. Conclusion

The EXAFS study of amorphous samples of the zone of glass formation of the ternary system Sb_2S_3–As_2S_3–Tl_2S shows that the environment of arsenic is, in all cases, of the pyramidal AsS_3E type with As–S distances varying from 0.228–0.230 nm.

Thus, arsenic obeys the "8-N" rule even in these compounds of rather complicated structure, where the next-nearest neighbours may be sulphur, antimony or thallium. It therefore seems to be justified to fix the number of nearest neighbours to 3 during the fitting routine, in order to obtain Debye–Waller factors of higher precision. This increased precision allows us to extract from the EXAFS data more reliable results on the local order around the arsenic atoms.

In this way it could be shown that the introduction of the glass-modifying thallium sulphide, Tl_2S, into the As_2S_3 host matrix breaks the As–S–As bridges and leads to non-bridging As–S bonds. Higher Debye–Waller factors and lower Fourier transform amplitudes reflect this increased disorder. The opposite effect may be achieved by introducing the glass-forming antimony sulphide, Sb_2S_3. In this case As–S–Sb bridges are formed. The decreasing Debye–Waller factor and As–S distance with increasing antimony concentration confirm the model of random substitution of arsenic by antimony in the Sb_2S_3–As_2S_3 system

rather than the model of completely separated pure As_2S_3 and Sb_2S_3 phases.

The study of the ternary system shows that both competitive effects – breaking of As–S–As bridges by thallium and formation of As–S–Sb bridges – occur simultaneously. As the ratio between bridging and non-bridging bonds influences the mechanical and thermal properties of the compounds, the variation of the Sb_2S_3 and Tl_2S concentrations offers the possibility to synthesize glasses with predetermined properties. Our conclusions on all vitreous systems were confirmed by other techniques such as XAS at the SbL_{III} and SK-edges [34, 35], and ^{121}Sb Mössbauer [36], infrared and Raman spectroscopies [37].

Acknowledgements

This research was carried out within the GDRE "CHALCOGENURES". The authors acknowledge helpful discussions with P. E. Lippens. We are grateful to M. L. Elidrissi Moubtassim and M. A. El Idrissi for providing and helping with the synthesis and experimental measurements.

References

1. J. S. SANGHERA, J. HEO and J. D. MACKENZIE, *J. Non-Cryst. Solids* **103** (1988) 155.
2. T. KATSUYAMA and H. MATSUMURA, *ibid.* **139** (1992) 177.
3. J. OLIVIER-FOURCADE, A. BOUAZA, J. C. JUMAS and M. MAURIN, *ibid.* **111** (1989) 277.
4. S. C. KATYAL and K. L. BHATAI, *J. Phys. Chem. Solids* **41** (1980) 821.
5. N. S. PLATAKIS, *J. Non-Cryst. Solids* **24** (1977) 365.
6. S. R. JAGTAP and J. K. ZOPE, *ibid.* **127** (1991) 19.
7. D. GOMEZ-VELA, L. ESQUIVIAS and C. PRIETO, *ibid.* **167** (1994) 59.
8. E. SAGBO, D. HOUPHOUET-BOIGNY, R. EHOLIE, J. C. JUMAS, J. OLIVIER-FOURCADE, M. MAURIN and J. RIVET, *J. Solid State Chem.* **112** (1994) 31.
9. J. C. PHILLIPS, *J. Non-Cryst. Solids* **34** (1979) 153.
10. *Idem*, *ibid.* **43** (1981) 37.
11. *Idem*, *Phys. Rev. B*, **36** (1987) 4265.
12. P. BOOLCHAND, R. N. ENZWEILER, R. L. CAPPELLETTI, W. A. KAMITAKAHARA, Y. CAI and M. F. THORPE, *Solid State Ionics* **39** (1990) 81.
13. A. C. WRIGHT, R. A. HULME, D. I. GRIMLEY, R. N. SINCLAIR, S. W. MARTIN, D. L. PRICE and F. L. GALEENER, *J. Non-Cryst. Solids* **129** (1991) 213.
14. Y. KAWAMOTO and S. TSUCHIHASHI, *Yogyo-Kyokai Shi* **7** (1969) 328.
15. K. WHITE, R. L. CRANE and J. A. SNIDE, *J. Non-Cryst. Solids* **103** (1988) 210.
16. L. TICHY, A. TRISKA, M. FRUMAR, H. TICHA and J. KLIKORKA, *ibid.* **50** (1982) 371.
17. E. BYCHKOV and G. WORTMANN, *ibid.* **159** (1993) 162.
18. A. MICHALOWICZ, "EXAFS pour le Mac", in Logiciels pour la Chimie, edited by Société Française de Chimie (Paris, 1991) p. 102.
19. B. LENGELER and P. EISENBERGER, *Phys. Rev. B* **21** (1980) 4507.
20. B. K. TEO and P. A. LEE, *J. Am. Chem. Soc.* **101** (1979) 2815.
21. A. G. McKALE, G. S. KNAPP and S. K. CHAN, *Phys. Rev. B* **33** (1986) 841.
22. D. J. E. MULLEN and W. NOWACKI, *Z. Kristallogr.* **136** (1972) 48.
23. V. DIVJAKOVIC and W. NOWACKI, *ibid.* **144** (1976) 323.
24. M. E. FLEET, *ibid.* **138** (1973) 147.
25. M. GOSTOJIC, *ibid.* **151** (1980) 249.
26. A. MICHALOWICZ, PhD thesis, Université Paris Val de Marne, France (1990).
27. A. M. FLANK, D. BAZIN, H. DEXPERT, P. LAGARDE, C. HERVO and J. Y. BARRAUD, *J. Non-Cryst. Solids* **91** (1987) 306.
28. C. Y. YANG, M. A. PAESLER and D. E. SAYERS, *Phys. Rev. B* **36** (1987) 980.
29. *Idem*, *ibid.* **36** (1987) 9160.
30. V. MASTELARO, H. DEXPERT, S. BENAZETH and R. OLLITRAULT-FICHET, *J. Solid. State Chem.* **96** (1992) 301.
31. V. MASTELARO, S. BENAZETH, H. DEXPERT, A. IBANEZ and R. OLLITRAULT-FICHET, *J. Non-Cryst. Solids* **151** (1992) 1.
32. M. OKUNO, H. SUGAYA and T. MATSUMOTO, *ibid.* **150** (1992) 356.
33. J. HEO, J. S. SANGHERA and J. MACKENSIE, *ibid.* **101** (1988) 23.
34. J. M. DURAND, P. E. LIPPENS, J. OLIVIER-FOURCADE, J. C. JUMAS and M. WOMES, *J. Non-Cryst. Solids* **194** (1996) 109.
35. *Idem*, *ibid.* **208** (1996) 36.
36. J. M. DURAND, M. A. EL IDRISSI RAGHNI, J. OLIVIER-FOURCADE, J. C. JUMAS and G. LANGOUCHE, *J. Solid State Chem.*, (submitted) 1996.
37. M. A. EL IDRISSI RAGHNI, J. M. DURAND, B. BONNET, L. HAFID, J. OLIVIER-FOURCADE and J. C. JUMAS, *J. Alloys Comp.* **239** (1996) 8.

Received 4 December 1995
and accepted 10 March 1997